Riccati Matrix Differential Equation Formulation for the Analysis of Nonuniform Multiple Coupled Microstrip Lines

Jen-Tsai Kuo, *Member, IEEE*

Abstract— **A Riccati matrix differential equation (RMDE) is formulated for analyzing nonuniform coupled microstrip lines (NCML's) in the frequency domain. The formulation is based on a reciprocity-related definition in the theory of multiconductor transmission lines under quasi-TEM assumption. The hybrid-mode nature of modal phase velocities and strip characteristic impedances for multiconductor microstrip structure is included. The nonlinear RMDE is first transformed into a first-order linear differential matrix equation which can be efficiently solved using method of moments. A convergence study is performed to investigate the sufficient number of basis functions used in the method. The voltage-scattering parameters of a tapered microstrip and two three-line structures are presented. The frequency responses of a pair of nonuniform coupled lines are measured and compared with calculated results.**

I. Introduction

NONUNIFORM coupled microstrip lines (NCML's) play an important role in both analog and digital microwave integrated circuits. Using NCML's, for example, a folded all-pass two-port network [1] and a directional coupler [1], [2] can be realized with high coupling values operating over an ultra-wide frequency band. To date, NCML's serve as the interconnections in most chip packages for digital integrated circuits of switching speed covering the microwave or millimeter-wave regime [3]–[9]. With the advances of today's semiconductor fabrication technology, the major portion of delay time in a microwave integrated circuit (MIC) can be due to these interconnection lines [3]. One possible way for reducing the delay time is to increase the density of the interconnecting NCML's. As the NCML's become shorter or are placed closer, the nonuniformity of the lines must be properly designed in order to obtain transmitted signals with sufficiently high quality.

When high-speed signal travels along NCML's, the received signal at the load end can be degraded due to 1) dispersion, 2) cross talk, 3) losses, and 4) reflections. The cross talk and dispersion are due to the differences of relative effective dielectric constants for different modes and at different frequencies, respectively. The losses which include conductor, dielectric, and radiation attenuation factors will lower the power level of the received signal. If the lines are electrically short and made on a low-loss substrate, the radiation can dominate the loss mechanism. Reflections are caused by the position-dependent impedance values along the lines. Note that all the aforesaid factors depend on the nonuniformity of the lines and on the operation frequency which make the characterization of the NCML's network become a complicated task.

Several methods have been developed to analyze multiple NCML's. Mehalic and Mittra [4] investigated the tapered multiple microstrip lines using a spatial iteration-perturbation approach technique. Oh and Schutt-Aine [5] analyzed the nonuniform lines based on a time-domain scattering parameter formulation incorporated with the closed-form expressions of voltage variables for divided short uniform lossless lines. Mao and Li proposed a method of convolution-characteristic [6] and a method of equivalent cascaded network chain [7] to handle the transient response of NCML's. Palusinski and Lee [3] used Chebyshev polynomials to expand the current and voltage along the nonuniform lines in the time-domain to predict the reflections and cross talk of general multiple coupled line systems.

In frequency domain, Arabi *et al.* [8] presented an electrical field integral equation formulation based on a combined approach of using closed-form near and far field approximations for the Sommerfeld microstrip Green's functions. The accuracy of this technique can be set to any desired value. In [9], Pan and his colleagues extended the method in [3] to the frequency domain. The advantages of analyzing NCML's in the frequency domain over the time domain were also discussed.

To calculate the input reflection coefficient matrix of terminated NCML's, we derive a differential matrix equation, which is known as the Riccati matrix differential equation (RMDE), based on a reciprocity-related definition of the line voltages and currents for hybrid-mode multiple coupled microstrips. The RMDE is expressed in terms of the normal mode parameters of coupled microstrips and solved by method of moments. The method of solution is also extended to calculate the scattering parameters of $2N$-port NCML's networks.

The presentation is organized as follows. Section II describes the background of the mathematical modeling of NCML's and lists the mathematical formulas to describe the reflection along the lines. Section III presents the method of solution to the nonlinear RMDE. In Section IV, the convergence behavior of the analysis method is investigated and

Manuscript received August 22, 1995; revised February 15, 1996. This work was supported in part by the National Science Council, Taiwan, Grant NSC 85-2213-E-009-002.

The author is with the Department of Communication Engineering, National Chiao Tung University, 1001 Ta-Hsueh Road, Hsinchu, Taiwan, R.O.C.

Publisher Item Identifier S 0018-9480(96)03783-0.

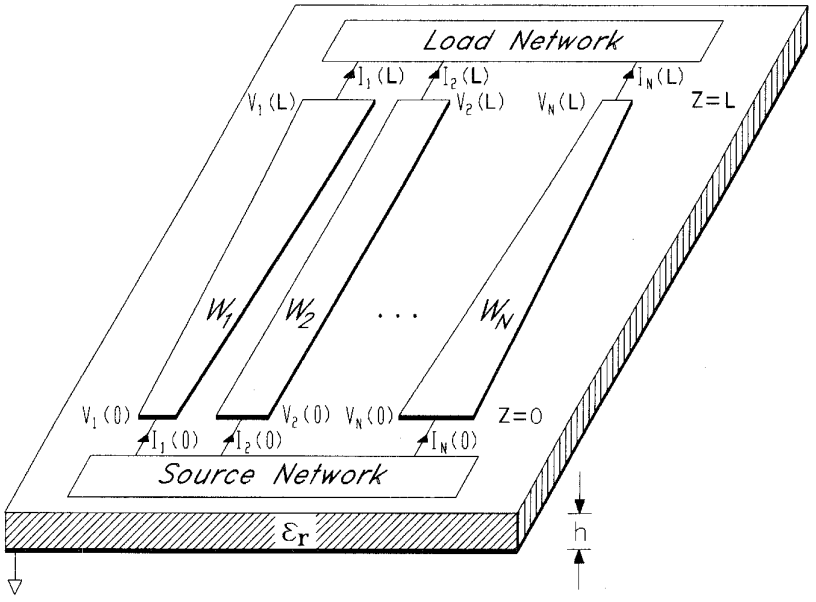

Fig. 1. A system of N-conductor nonuniform coupled microstrip lines.

several numerical aspects are discussed. Numerical results for certain nonuniform single microstrip and three-line structures are presented and discussed. Section V compares the measured frequency responses of a nonuniform two-line structure with the calculated results. Finally, Section VI draws the conclusion.

II. The Riccati Matrix Differential Equation (RMDE)

It is known that a system of uniform N-conductor coupled microstrip lines and a ground line support N dominant or quasi-TEM modes. For the NCML's in Fig. 1, we neglect the fringing fields, which produces radiation loss, caused by the gradual change of waveguide cross section. For lines with abrupt discontinuities, field-theoretical oriented formulations, such as that in [8], can be referred to enhance accuracy of results. At any z along the NCML's, through the full-wave solution, an $N \times N$ matrix $[M_I]$, called the eigencurrent matrix, can be obtained [10]. Of $[M_I]$ each column vector consists of total currents on the lines for a given mode. Based on the orthogonality of modal voltage and current vectors, an eigenvoltage matrix $[M_V]$ is uniquely defined [11]. For each mode, inner product of the eigenvoltage and eigencurrent vectors is set to be the total electromagnetic power transfer. This is an important fact that leads our field problem to be able to be formulated by circuit quantities.

The characteristic admittance matrix along the lines is given by [11]

$$[Y_C] = [M_I][M_V]^{-1}. \tag{1}$$

It can be shown that $[Y_C]$ is symmetric and the important aspect of reciprocity is guaranteed. If the load network has an admittance matrix identical to the $[Y_C]$ of the NCML's at the load end, then there is no reflection.

The equivalent distributed capacitance matrix $[C]$ and inductance matrix $[L]$ along the lines can be derived [10]

$$[C] = [M_I]\,\mathrm{diag}\,(\beta_k/\omega)[M_V]^{-1} \tag{2}$$

$$[L] = [M_V]\,\mathrm{diag}\,(\beta_k/\omega)[M_I]^{-1} \tag{3}$$

where ω is the angular frequency and β_k is the phase constant of the kth mode. Note that all the entries in $[M_I]$, $[M_V]$, $[Y_C]$, $[L]$, and $[C]$ are dispersive and position-varying along the NCML's. Let $[I]$ and $[V]$ be the line current and line voltage column vectors of which the kth entries are the total current and voltage on the kth line, respectively. Then, from the multiconductor transmission-line theory [3]

$$[I] = [Y_{in}][V] \tag{4}$$

$$[V]' = -[Z][I] \tag{5}$$

$$[I]' = -[Y][V] \tag{6}$$

where $[Y_{in}]$ is the input admittance matrix seen at z toward the load, $[Z]$ and $[Y]$ are, respectively, the series impedance and shunt admittance matrices per unit length of the NCML's, and the prime ($'$) represents the derivative with respect to z. If the tapered lines are lossless, $[Z] = j\omega[L]$ and $[Y] = j\omega[C]$. Let the reflection coefficient matrix along the longitudinal direction be $[\rho_V]$, then $[Y_{in}]$ and $[\rho_V]$ are related by [10]

$$[Y_{in}] = [Y_C]([U] - [\rho_V])([U] + [\rho_V])^{-1} \tag{7}$$

where $[U]$ is the identity matrix of size $N \times N$. Substitution of (4) and (5) into (6) leads to

$$[Y_{in}]' - [Y_{in}][Z][Y_{in}] + [Y] = 0. \tag{8}$$

Inserting (7) into (8), one obtains

$$[\rho_V]' = j([\gamma][\rho_V] + [\rho_V][\gamma]) + ([U] + [\rho_V])[G]([U] - [\rho_V]) \tag{9}$$

where $[\gamma] = [Y_C]^{-1}[Y] = [Z][Y_C] = [M_V]\,\mathrm{diag}\,(\beta_k)[M_V]^{-1}$ and $[G] = [Y_C]^{-1}[Y_C]'/2$. Note that (8) and (9) are known as the RMDE [12] which is nonlinear. It is believed that [13] is the first literature that formulated the RMDE (8) for studying general nonuniform transmission lines.

In the case of single nonuniform line, (9) becomes the Riccati scalar differential equation (RSDE) [12]. To simplify this nonlinear differential equation, many authors [14–16] neglected the ρ_v^2 term. The solution of ρ_v at $z = 0$ can then be obtained through a simple Fourier transform of a function of the line characteristic impedance. Based on the transform, synthesis of matching transformers and couplers using nonuniform transmission lines have been developed [15], [16]. Note that the legitimacy of the negligence is relied on the fact that $\rho_v^2 \ll 1$ along the line. Thus, an error in ρ_v will be generated at low frequencies for lines used to match impedances with large ratio. The following section formulates the method of solution to (9) in which no such error will occur.

III. Method of Solution

It is found that the RMDE can always be transformed into a linear equation [12]. This can be done by defining

$$\begin{bmatrix} D \\ R \end{bmatrix}' = \begin{bmatrix} A_{11} & A_{12} \\ A_{21} & A_{22} \end{bmatrix} \begin{bmatrix} D \\ R \end{bmatrix} \tag{10}$$

where $[A_{12}] = [A_{21}] = [G]$ and $[A_{22}] = [A_{11}]^* = j[\gamma] - [G]$ for lossless NCML's. The asterisk denotes the complex conjugate operation. It has been shown in [12] that if $[D]$ and $[R]$ satisfy (10) then

$$[\rho_V] = [R][D]^{-1} \tag{11}$$

is the solution to (9) provided that $[D]$ is nonsingular for all z. The matrix equation (10) can be rewritten as

$$[X]' = [A][X] \tag{12}$$

where $[X] = [D^{\mathrm{T}} R^{\mathrm{T}}]^{\mathrm{T}}$ and the superscript T stands for the transpose operation. It is interesting to note that if $[V]$ and $[I]$ in (4) through (6) are replaced by

$$[V] = [V^+] + [V^-] \tag{13}$$

$$[I] = [Y_C]([V^+] - [V^-]) \tag{14}$$

where $[V^+]$ and $[V^-]$ are the forward and backward traveling voltage wave vectors along the NCML's, then one can find that $[V^{\pm}] = [V^{+\mathrm{T}} V^{-\mathrm{T}}]^{\mathrm{T}}$ also satisfies (12). In other words, the nonsingular matrix $[D]$ consists of N linearly independent $[V^+]$s as its column vectors and $[R]$ consists of the corresponding $N[V^-]$ vectors.

Analytical solution to (12) is difficult or impossible to obtain since the eigenvalues and eigenvectors of the complex matrix function $[A]$ are position-dependent [17]. To solve (12), we use the method of moments which is closely related to the case of a single nonuniform line in [18]. $[A]$ and $[X]$ are expanded as

$$[A] = \sum_{m=0}^{M_1} [A_m] z^m \tag{15}$$

$$[X] = \sum_{m=0}^{M_2} [X_m] C_m(z) \tag{16}$$

where $C_m(z)$ is the shifted Chebyshev polynomial of order m of the first kind defined over $0 \le z \le L$, L being the length of the NCML's, and $[X_m]$ and $[A_m]$ are constant matrices. The matrix $[A]$ is first expanded into a linear combination of $C_m(z)$ of which each coefficient matrix can be obtained by Gaussian Chebyshev quadratures [19]. Then $[A_m]$s can be obtained since each $C_m(z)$ is known as a polynomial of z of degree m. Following the method in [20], more precisely the Galerkin procedure in method of moments, one can obtain

$$[X] \approx [Q][X(L)] \tag{17}$$

and

$$[Q]^{-1} = [U] + \sum_{m=0}^{M_1} [A_m] \otimes ([P][H]^m) \tag{18}$$

where $[U]$ is the identity matrix of size $2N(M_2+1)\times 2N(M_2+1)$. $[P]$ and $[H]$ are the operation matrices of integration and of z-multiplication, respectively, of the shifted Chebyshev polynomials. They are given by

$$[P] = \begin{bmatrix} \lambda_0 & \lambda_1 & \lambda_2 & \lambda_3 & & \lambda_{N-1} & \lambda_N \\ -\alpha_0 & 0 & -\eta_2 & 0 & & 0 & 0 \\ 0 & -\alpha_1 & 0 & -\eta_3 & \cdots & 0 & 0 \\ 0 & 0 & -\alpha_2 & 0 & & \vdots & \vdots \\ 0 & 0 & 0 & -\alpha_3 & & -\eta_{N-1} & 0 \\ \vdots & \vdots & \vdots & \vdots & & 0 & -\eta_N \\ 0 & 0 & 0 & 0 & & -\alpha_{N-1} & 0 \end{bmatrix} \tag{19}$$

and

$$[H] = (L/2)[H_o] \tag{20}$$

where $\alpha_o = L/2$, $\alpha_k = L/4(k+1)$ for $k \ge 1$, $\eta_o = \eta_1 = 0$, $\eta_k = L/4(1-k)$ for $k \ge 2$, and $\lambda_k = \alpha_k + \eta_k$ for $k \ge 0$. $[H_o]$ is a tridiagonal matrix with all diagonal entries and the $(2, 1)$th one being 1 and all the other nonzero entries being 0.5.

In (18), $\otimes$ denotes the Kronecker product, defined as

$$[A] \otimes [B] = \begin{bmatrix} [A]B(1,1) & [A]B(1,2) & \cdots & [A]B(1,k) \\ [A]B(2,1) & [A]B(2,2) & \cdots & [A]B(2,k) \\ \vdots & \vdots & & \vdots \\ [A]B(1,1) & [A]B(1,2) & \cdots & [A]B(k,k) \end{bmatrix}. \tag{21}$$

Note that only the entries in the first $2N$ columns in $[Q]$ are useful in calculating the network parameters since $[X(L)] = [D(L)^{\mathrm{T}} R(L)^{\mathrm{T}} 0\ 0 \cdots 0]^{\mathrm{T}}$. If $[Q]$ is partitioned into $2(M_2+1) \times 2(M_2+1)$ submatrices $[q]_{ij}$, of each the size is $N \times N$, then it can be readily shown that

$$[V^+(0)] = [\Delta_{11}][V^+(L)] + [\Delta_{12}][V^-(L)] \tag{22}$$

$$[V^-(0)] = [\Delta_{21}][V^+(L)] + [\Delta_{22}][V^-(L)] \tag{23}$$

with

$$[\Delta_{ij}] = \sum_{m=0}^{M_2} (-1)^m [q]_{2m+i,\,j}, \qquad i, j = 1 \text{ or } 2. \tag{24}$$

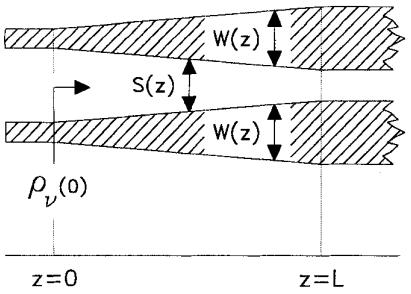

Fig. 2. Planar view of the nonuniform coupled microstrips for investigating convergence behavior of the method. The load is assumed perfectly matched. $W(z) = 0.36 + 0.84(z/L)$ mm, $S(z) = 1.8 - W(z)$ mm, $L = 10$ mm. The dielectric substrate has $\epsilon_r = 12.9$ and height $h = 1$ mm.

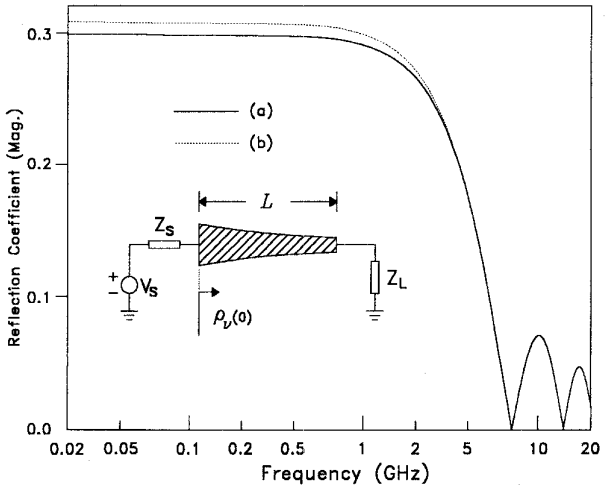

Fig. 3. Comparison of the input reflection coefficients of an exponential microstrip taper on a substrate with $\epsilon_r = 8$ designed for transforming $Z_S = 63.58\ \Omega$ to $Z_L = 117.99\ \Omega$, $L = 9h = 9$ mm. Response (a) is the complete solution to the RSDE and (b) is that to the RSDE with the ρ_v^2 term being omitted. The width profile of the tapered microstrip see [16, Fig. 7]. The line characteristic impedances use dc values.

Following the voltage scattering parameter matrices used in [21] and defining

$$\begin{bmatrix}[V^-(0)]\\ [V^+(L)]\end{bmatrix} = \begin{bmatrix}[S_{11}] & [S_{12}]\\ [S_{21}] & [S_{22}]\end{bmatrix}\begin{bmatrix}[V^+(0)]\\ [V^-(L)]\end{bmatrix} \tag{25}$$

one can obtain

$$[S_{11}] = [\Delta_{21}][\Delta_{11}]^{-1} \tag{26a}$$

$$[S_{12}] = [\Delta_{22}] - [\Delta_{21}][\Delta_{11}]^{-1}[\Delta_{12}] \tag{26b}$$

$$[S_{21}] = [\Delta_{11}]^{-1} \tag{26c}$$

$$[S_{22}] = -[\Delta_{11}]^{-1}[\Delta_{12}]. \tag{26d}$$

The voltage scattering parameter matrices can be used to characterize the $2N$-port NCML's network for any linear time-invariant termination conditions at both the source and the load ends. However, (22) and (23) are still useful in calculating some important network parameters. For example, when $[\rho_V(L)]$ exists at the load end, then the input reflection matrix can be found as

$$[\rho_V(0)] = ([\Delta_{21}] + [\Delta_{22}][\rho_V(L)]) \cdot([\Delta_{11}] + [\Delta_{12}][\rho_V(L)])^{-1} \tag{26}$$

TABLE I
CONVERGENCE ANALYSIS OF THE PROPOSED METHOD

$\lvert[\rho_V(0)](1,1)\rvert\times10^2 = \lvert[\rho_V(0)](2,2)\rvert\times10^2$							
M_2 \ M_1	4	5	6	7	8	9	10
4	2.0353	2.0353	2.0379	2.0385	2.0385	2.0386	2.0387
6	1.9514	1.9318	1.9325	1.9325	1.9325	1.9322	1.9320
8	1.9569	1.9364	1.9370	1.9379	1.9379	1.9379	1.9379
10	1.9569	1.9359	1.9365	1.9375	1.9375	1.9376	1.9376
12	1.9569	1.9360	1.9365	1.9375	1.9375	1.9376	1.9376
$\lvert[\rho_V(0)](1,2)\rvert\times10^2 = \lvert[\rho_V(0)](2,1)\rvert\times10^2$							
M_2 \ M_1	4	5	6	7	8	9	10
4	1.0058	1.0058	1.0076	1.0074	1.0074	1.0074	1.0075
6	1.0936	1.1008	1.1004	1.1004	1.1005	1.1006	1.1003
8	1.0890	1.0968	1.0969	1.0965	1.0966	1.0966	1.0966
10	1.0891	1.0970	1.0971	1.0967	1.0967	1.0967	1.0967
12	1.0891	1.0970	1.0971	1.0967	1.0967	1.0967	1.0967

IV. RESULTS

A. The Database of NCML's Normal Mode Parameters

To calculate the $2N$-port parameters of NCML's, we use spectral domain approach (SDA) [10] to evaluate the normal mode parameters. For all NCML's addressed in this paper, the evaluations are sampled at $z_m = mL/20$, $m = 0(1)20$, with L being the length of lines, for frequencies at $0.5n$ GHz, $n =$ integer. At each frequency point, each entry of $[\gamma]$ and $[G]$ in (9) is approximated by a cubic spline interpolation for use in the numerical quadrature for finding $[A_m]$s in (15).

B. Convergence Study and Some Numerical Aspects

Table I shows convergence behavior of the input reflection coefficients $[\rho_V(0)]$ for a tapered two-line structure of which the planar geometry is drawn in Fig. 2. The even- and odd-modes are found to have relative effective dielectric constants close to 9, thus the length of lines is about one guided wavelength for both modes at 10 GHz. Note that, due to the structural symmetry, $|[\rho_V(0)](2, 2)| = |[\rho_V(0)](1, 1)|$ and $|[\rho_V(0)](2, 1)| = |[\rho_V(0)](1, 2)|$.

In Table I, the listed results are according to values of M_1 (See (15)) and M_2 (See (16)) ranging from 4 to 10 and from 4 to 12, respectively. The execution CPU time is dominated by M_2 for setting up the matrix $[Q]$ in (18). For both the (1, 1)th and (1, 2)th values, it shows that using $M_2 = 4$ produces results with errors with several percents. For $M_2 \geq 8$, when M_1 is increased from 6 to 10, both sets of the reflection values converge to at least four significant digits. According to our experience, to have the same converged results at 20 GHz, it requires $M_1 = M_2 = 12$.

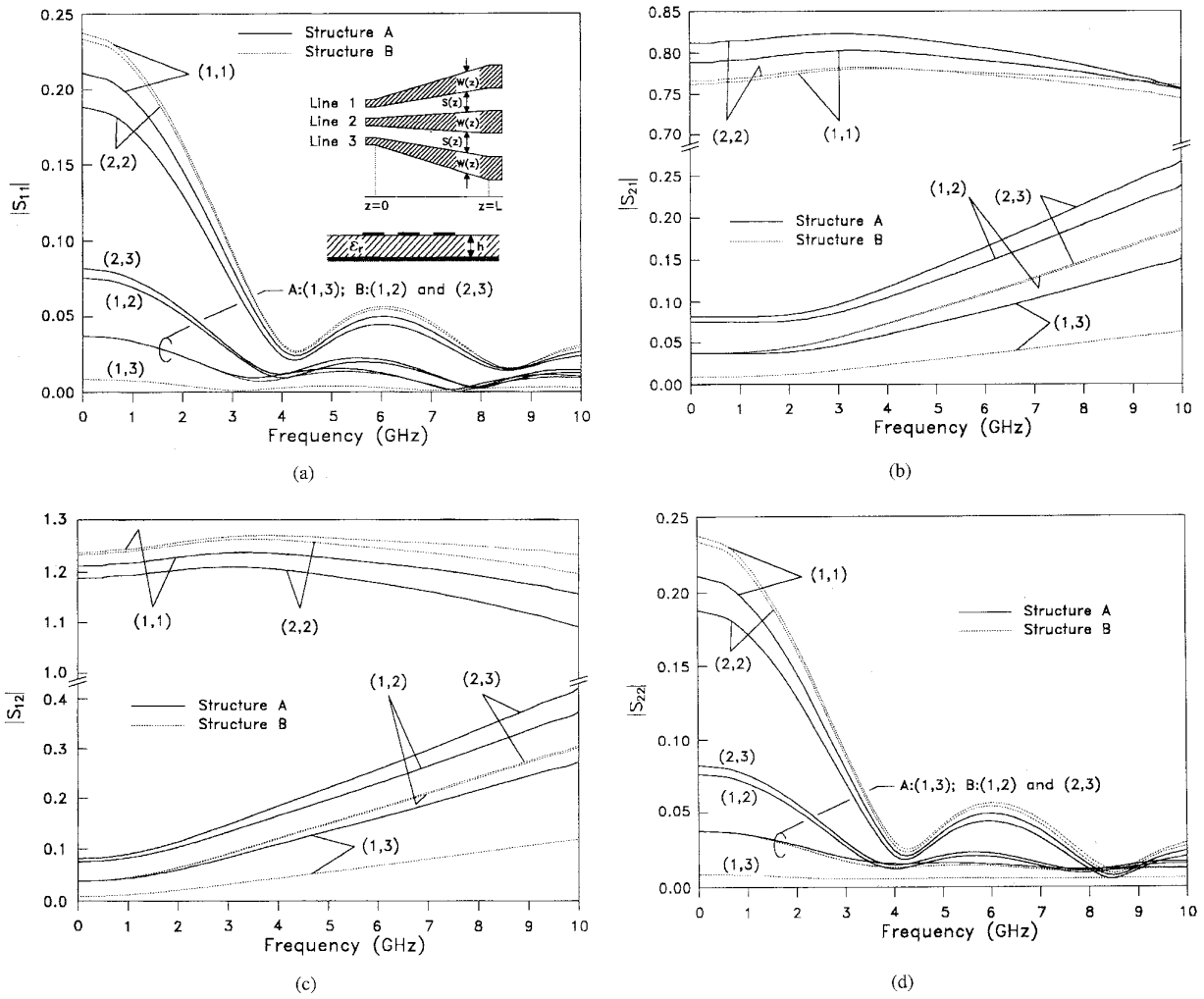

Fig. 4. The voltage-scattering parameters for two tapered three-line microstrips. $h = 0.508$ mm, $\epsilon_r = 4.2$, $W(z) = W_o(1 + 2z/L)$, $W_o = 0.24$ mm, and $L = 20$ mm. $S(z) = 0.5W_o(1 + z/L)$ for structure A and $S(z) = 2.5W_o(1 + z/L)$ for structure B. (a) $|S_{11}|$. (b) $|S_{21}|$. (c) $|S_{12}|$. (d) $|S_{22}|$.

C. The Input Reflection Coefficient for a Tapered Microstrip

To calculate the reflection coefficient of a nonuniform microstrip, the Riccati scalar differential equation (RSDE) reduced from (9) can be invoked. When the ρ_V^2 term is omitted in the equation, it is equivalent in our method of solution to enforce that $[A_{12}] = 0$ and $[A_{22}] = [A_{11}]^* = j[\gamma]$ (See (10)). Therefore it is easy to investigate the effectiveness of the negligence of the ρ_v^2 term on the results using our readily developed program. We use an exponential microstrip taper, of which the z-dependent width profile is in [16, Fig. 7], as the test structure. The line characteristic impedances use the dc values. The length of the line is 9 mm which corresponds to $L/\lambda_o = 0.6$ at 20 GHz.

The taper is designed for transforming $Z_L = 117.99\ \Omega$ to $Z_S = 63.58\ \Omega$. So the reflection coefficient at dc is $(Z_L - Z_S)/(Z_L + Z_S) \approx 0.3$. In Fig. 3, the solid and dotted responses compare the solutions to the RSDE with and without the ρ_v^2 term. Both curves agree very well for frequencies higher than 3 GHz, at which the line is about one fifth of guided wavelength. The values of $|\rho_v(0)|$ for both cases have a deviation of 3% for frequencies less than 1 GHz where the value of $\rho_v(z)$ remains nearly constant (0.3) all over the line. It is believed that the influence of neglecting the ρ_v^2 term on the solution to the RSDE for analyzing tapered microstrip is reported for the first time.

D. The $2N$-Port Network Parameters for Tapered Three-Line Structures

Fig. 4 compares responses for two tapered three-line structures with the same line width geometry but different line spacing. The solid lines represent the parameters for structure A which has smaller line spacing. More interline coupling or cross talk voltage level is expected for structure A than B. Again, due to the structural symmetry, only five entries of each S-parameter matrix need specifying.

Before we look into details on the $2N$-port parameters of the NCML's, let us review certain important formulas that can help understanding of the results. The S-parameters we use here are based on the voltage wave instead of power wave definition. Thus, at zero frequency, the $[S_{11}]$ and $[S_{21}]$

are, respectively, the reflection ($[\rho_V]$) and transmission ($[T_V]$) coefficient matrices of a step impedance junction with source admittance matrix $[Y_C(0)]$ and load $[Y_C(L)]$, i.e., [10]

$$[\rho_V] = ([Y_C(0)] + [Y_C(L)])^{-1}([Y_C(0)] - [Y_C(L)]) \quad (27)$$

and

$$[T_V] = 2([Y_C(0)] + [Y_C(L)])^{-1}[Y_C(0)]. \quad (28)$$

The results of $[S_{12}]$ and $[S_{22}]$ matrices at dc can be known in a similar fashion. For closely packed symmetrical three-line microstrip [10], $[Y_C](2, 2) < [Y_C](1, 1) = [Y_C](3, 3)$ and the diagonal elements of $[Y_C]$ decrease as the line spacing is decreased. Thus, the $[Y_C](k, k)$, $k = 1$, 2, and 3, for structure A are smaller than those for B.

Fig. 4(a) compares the $|S_{11}|$ responses. For each structure, entry (1, 1) is larger than entry (2, 2). It means that, when the lines are perfectly terminated at the load end, the relative reflection at line 1 due to an excitation at line 1 is larger than that at line 2 due to an excitation at line 2. Entries (1, 1) and (2, 2) for structure B, which has smaller interline coupling, have closer and larger values than those for structure A. However, entries (1, 2), (2, 3), and (1, 3) for B are smaller than those for A.

The forward transmission coefficient or $|S_{21}|$ responses are plotted in Fig. 4(b). Structure A has larger entry values than B. The (1, 1) and (2, 2) values are firstly increased at lower frequencies and reach their maxima at about 4 GHz, where the $|S_{11}|$ entries have their minima, then decrease as frequency is further increased due to the increase of magnitudes of entries (1, 2), (2, 3), and (1, 3). These three entries can be interpreted as the "cross talk" for this NCML's structure.

The $|S_{12}|$ responses are shown in Fig. 4(c). The relative cross talk voltage levels are larger than those for $|S_{21}|$ entries. Note that these cross talk voltage levels are not zero at dc. This can be explained from (28). Entries (1, 1) and (2, 2) for structure B are larger than those for structure A.

The $|S_{22}|$ responses are plotted in Fig. 4(d). According to (27), the $|S_{22}|$ entries should have nearly the same magnitudes as the corresponding ones of $|S_{11}|$ at lower frequencies.

D. Experimental Measurements

We measure the responses of a pair of symmetrical nonuniform coupled microstrips of which the planar view is shown in Fig. 5(a). At both ends of the circuit, the line width is chosen to have 50 Ω characteristic impedance and the spacing is 3.5 times the width so that the interline coupling can be neglected [10]. The test circuit is fabricated on a low-loss alumina substrate ($\epsilon_r = 9.9$, loss tangent tan $\delta \leq 0.001$). A TaN (Tantalum Nitride) thin film resistive layer, sandwiched between the substrate and metal, can be used for termination design. The termination resistance value should be carefully trimmed during the fabrication process since improper termination condition will cause unwanted reflections.

The measurement is performed using the HP8510B network analyzer and the results are shown in Fig. 5(b). The agreement between the calculated and measured $|S_{11}|$ responses is fairly good. The predicted $|S_{21}|$ response, however, begins to deviate

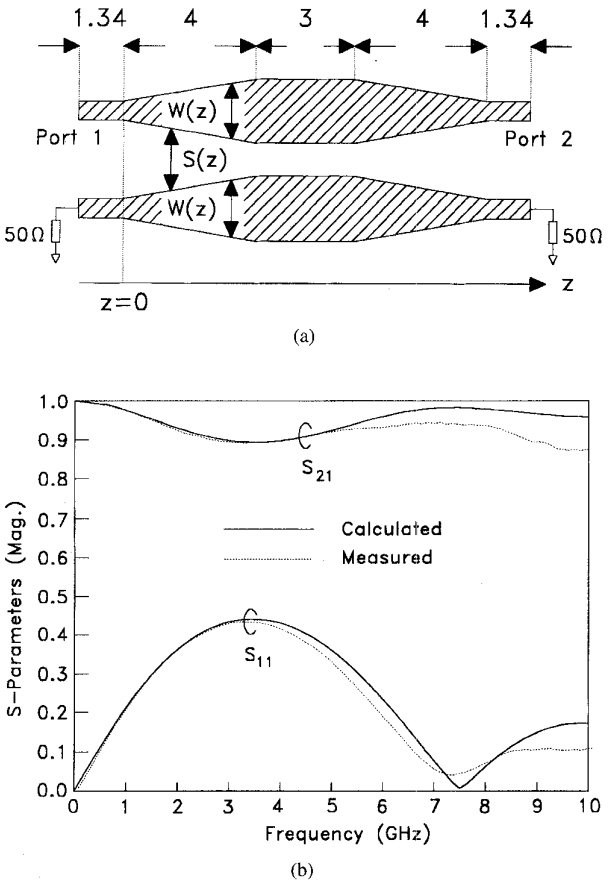

Fig. 5. The results for the experimental nonuniform coupled microstrips. $\epsilon_r = 9.9$, $h = 0.254$ mm, $W_1 = 0.254$ mm, $W_2 = 0.635$ mm, $S_1 = 0.889$ mm, $S_2 = 0.508$ mm, $W(z) = W_1 + (W_2 - W_1)z/4$, and $S(z) = S_1 + (S_2 - S_1)z/4$. The structure is symmetric about $z = 5.5$ mm. (a) Circuit geometry. (b) Measured and calculated responses.

from the experimental results at 5 GHz where the length of line is about one half guided wavelength. The deviation could be caused by dielectric (α_d), conductor (α_c), and radiation losses. Similar deviation is also reported for a tapered three-line structure [4], where the fitness of prediction and measurement can be made up at lower frequencies by including the α_d and α_c factors, but the radiation loss is still significant at the higher frequency end. Note that the electrical length of the test circuit in Fig. 5 is only about one sixteenth of that used in [4]. According to our experience of designing multiple coupled microstrip lines on alumina substrate [10], the attenuation factor including α_d and α_c is approximately 0.01 dB/mm. Thus α_d and α_c could have only limited contribution to the deviation in our experiment and the deviation should be mainly due to the radiation caused by the line width nonuniformity.

V. Conclusion

A RMDE has been formulated for calculating the $2N$-port network parameters of nonuniform multiple coupled microstrips. The influence of neglecting ρ_V^2 term in the Riccati scalar differential equation on the input reflection coefficient response of a microstrip taper is investigated. From the in-

vestigation of two tapered three-line microstrips, the smaller is the line spacing or the higher is the operation frequency, the higher is the crosstalk level. From the experimental two-line structure, the calculated and measured results agree well at lower frequencies and start to deviate at the frequency at which the radiation loss, due to the line width nonuniformity, becomes important.

ACKNOWLEDGMENT

The author would like to thank the Microelectronic Technology Inc., Hsinchu, Taiwan, for their support in fabricating the measured circuits and to T.-Y. Wu in ERSO, Hsinchu, Taiwan, for his help in the measurement works.

REFERENCES

[1] S. Yamamoto, T. Azakami, and K. Itakura, "Coupled nonuniform transmission line and its applications," *IEEE Trans. Microwave Theory Tech.*, vol. MTT-15, pp. 220–231, Apr. 1967.

[2] S. Uysal and H. Aghvami, "Synthesis, design, and construction of ultra-wide-band nonuniform quadrature directional couplers in inhomogeneous media," *IEEE Trans. Microwave Theory Tech.*, vol. 37, pp. 969–976, June 1989.

[3] O. A. Palusinski and A. Lee, "Analysis of transients in nonuniform and uniform multiconductor transmission lines," *IEEE Trans. Microwave Theory Tech.*, vol. 37, pp. 127–138, Jan. 1989.

[4] M. A. Mehalic and R. Mittra, "Investigation of tapered multiple microstrip lines for VLSI circuits," *IEEE Trans. Microwave Theory Tech.*, vol. 38, pp. 1559–1567, Nov. 1990.

[5] K. S. Oh and J. E. Schutt-Aine, "Transient analysis of coupled, tapered transmission lines with arbitrary nonlinear terminations," *IEEE Trans. Microwave Theory Tech.*, vol. 41, pp. 268–273, Feb. 1993.

[6] J. Mao and Z. Li, "Analysis of the time response of multiconductor transmission lines with frequency-dependent losses by the method of convolution-characteristics," *IEEE Trans. Microwave Theory Tech.*, vol. 40, pp. 637–644, Apr. 1992.

[7] ——, "Analysis of the time response of nonuniform multiconductor transmission lines with a method of equivalent cascaded network chain," *IEEE Trans. Microwave Theory Tech.*, vol. 40, pp. 948–954, May 1992.

[8] T. R. Arabi, A. T. Murphy, and T. K. Sarkar, "Electrical field integral equation formulation for a dynamic analysis of nonuniform microstrip multi-conductor transmission lines," *IEEE Trans. Microwave Theory Tech.*, vol. 40, pp. 1857–1869, 1992.

[9] G. Pan, G. J. Wunsch, and B. K. Gilbert, "Frequency-domain analysis of coupled nonuniform transmission lines using Chebyshev Pseudo-spatial technique," *IEEE Trans. Microwave Theory Tech.*, vol. 40, pp. 2025–2033, Nov. 1992.

[10] J.-T. Kuo and C.-K. C. Tzuang, "A termination scheme for high-speed pulse propagation on a system of tightly coupled coplanar strips," *IEEE Trans. Microwave Theory Tech.*, vol. 42, pp. 1008–1015, June 1994.

[11] L. Wiemer and R. H. Jansen, "Reciprocity related definition of strip characteristic impedance for multiconductor hybrid-mode transmission lines," *Microwave Opt. Tech. Lett.*, vol. 1, pp. 22–25, Mar. 1988.

[12] W. T. Reid, *Riccati Differential Equations*. New York: Academic, 1972.

[13] R. L. Sternberg and H. Kaufman, "Applications of the theory of systems of differential equations to multiple nonuniform transmission lines," *J. Math. and Phys.* vol. 31, pp. 244–252, 1952.

[14] R. W. Klopfenstein, "A transmission line taper of improved design," *Proc. IRE*, vol. 44, pp. 31–35, Jan. 1956.

[15] D. Pramanick and P. Bhartia, "A generalized theory of tapered transmission line matching transformers and asymmetric couplers supporting non-TEM modes," *IEEE Trans. Microwave Theory Tech.*, vol. 37, pp. 1184–1191, Aug. 1989.

[16] M. Kobayashi and N. Sawada, "Analysis and synthesis of tapered microstrip transmission lines," *IEEE Trans. Microwave Theory Tech.*, vol. 40, pp. 1642–1646, Aug. 1992.

[17] S. Amari, "Comments on 'An exact solution for the nonuniform transmission line problem," *IEEE Trans. Microwave Theory Tech.*, vol. 39, pp. 611–612, Mar. 1991.

[18] R. F. Harrington, *Field Computation by Moment Methods*. New York: Macmillan, 1968.

[19] H. Engels, *Numerical Quadrature and Cubature*. London: Academic, 1980.

[20] T. Lee and S. Tsay, "Analysis, parameter identification and optimal control of time-varying system via general orthogonal polynomials," *Int. J. System Sci.*, vol. 20, pp. 1451–1465, 1989.

[21] C. R. Paul, *Analysis of Multiconductor Transmission Lines*. New York: Wiley, 1994, ch. 8.

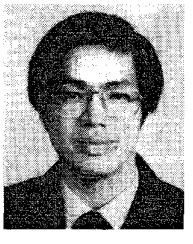

Jen-Tsai Kuo (S'89–M'93) received the B.S. degree in communication engineering from the National Chiao Tung University (NCTU) in 1981, the M.S. degree in electrical engineering from the National Taiwan University in 1984, and the Ph.D. degree from the Institute of Electronics, NCTU in 1992, all in Taiwan.

Since 1984, he has been with the Department of Communication Engineering at the NCTU as a Lecturer at both the Microwave and Communication Electronics Laboratories. Since 1995, he has been a Visiting Scholar at the University of California at Los Angeles. His research interests include the analysis and design of high-frequency electronic and microwave circuits, high-speed interconnects and packages, field-theoretical studies of guided waves, and numerical techniques in electromagnetics.